

Luminescent Cyclometalated Alkynylgold(III) Complexes with 6-Phenyl-2,2'-Bipyridine Derivatives: Synthesis, Characterization, Electrochemistry, Photophysics, and Computational Studies

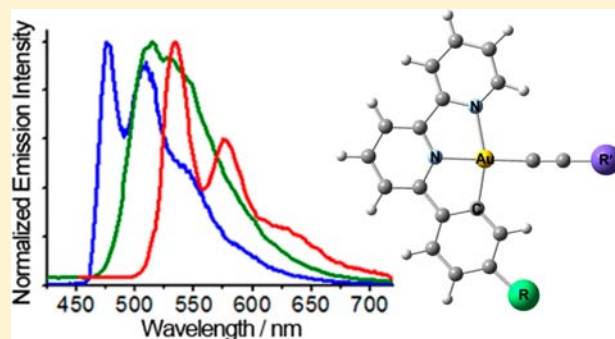
Vonika Ka-Man Au,^{†,‡} Wai Han Lam,^{†,‡} Wing-Tak Wong,[‡] and Vivian Wing-Wah Yam^{*,†,‡}

[†]Institute of Molecular Functional Materials (Areas of Excellence Scheme, University Grants Committee (Hong Kong)) and

[‡]Department of Chemistry, The University of Hong Kong, Pokfulam Road, Hong Kong, P.R. China

Supporting Information

ABSTRACT: A novel class of luminescent gold(III) complexes containing various tridentate cyclometalating ligands derived from 6-phenyl-2,2'-bipyridine and alkynyl ligands, $[\text{Au}(\text{RC}^{\wedge}\text{N}^{\wedge}\text{N})(\text{C}\equiv\text{C}-\text{R}')]\text{PF}_6$, has been successfully synthesized and characterized. One of the complexes has also been determined by X-ray crystallography. Electrochemical studies show a ligand-centered reduction originated from the cyclometalating $\text{RC}^{\wedge}\text{N}^{\wedge}\text{N}$ ligands as well as an alkynyl-centered oxidation. The electronic absorption and photoluminescence properties of the complexes have also been investigated. In acetonitrile at room temperature, the complexes show intense absorption at higher energy region with wavelength shorter than 320 nm, and a moderately intense broad absorption band at 374–406 nm, assigned as the metal-perturbed intraligand $\pi-\pi^*$ transition of the cyclometalating $\text{RC}^{\wedge}\text{N}^{\wedge}\text{N}$ ligand, with some charge transfer character from the aryl ring to the bipyridine moiety. Most of the complexes have been observed to show vibronic-structured emission bands at 469–550 nm in butyronitrile glass at 77 K, assigned to an intraligand excited state of the $\text{RC}^{\wedge}\text{N}^{\wedge}\text{N}$ ligand, with some charge transfer character from the aryl to the bipyridine moiety. Insights into the origin of the absorption and emission have also been provided by density functional theory (DFT) and time-dependent density functional theory (TDDFT) calculations.



INTRODUCTION

Transition metal complexes have attracted enormous attention over the past few decades in the area of materials science, especially for their applications as functional materials. An interesting property is related to their rich spectroscopic and luminescence behavior.¹ In particular, the chemistry of gold complexes represents an area of intensive research.^{1b,2–12} To search for new functional materials, one important way is to make use of transition metal complexes to develop novel photoluminescent materials that could be employed for a wide range of applications, ranging from optics,^{13,14} photonics,^{15,16} electronics,¹⁶ light-emitting devices,¹⁷ sensors,^{18,19} biolabels,²⁰ imaging agents,²¹ nanomaterials,²² to nanomedicines.^{23,24} In striking contrast to the related gold(I)^{2–12} and the isoelectronic platinum(II)¹ systems which have been extensively studied for their luminescence behavior, limited reports have been published on luminescent gold(III) complexes,^{7b} which probably stems from the presence of deactivating low-energy d-d ligand field (LF) states and the electrophilicity observed for the gold(III) metal center.^{7b} To enhance the luminescence of the gold(III) system, one strategy would be to introduce strong σ -donating ligands into the gold(III) center to render it more electron-rich, as first demonstrated by our group on stable gold(III) aryl complexes which were found to emit at both

ambient and low temperatures.²⁵ Extension of the work to the use of rigid cyclometalating ligands with strongly σ -donating alkynyl^{26,27} and *N*-heterocyclic carbene²⁸ ligands has been made to successfully prepare new classes of gold(III) complexes that display rich luminescence behavior at both room and low temperatures in various media. To further investigate and to tune the luminescence properties of the gold(III) system, it would be interesting to incorporate different classes of cyclometalating ligands into the gold(III) metal center, so as to vary the energy of the frontier molecular orbitals to produce metal complexes with different emission energies and/or origins. Apart from the tridentate 2,6-diphenylpyridine ($\text{C}^{\wedge}\text{N}^{\wedge}\text{C}$) derivatives^{26,28} and the bidentate 2-phenylpyridine ($\text{C}^{\wedge}\text{N}$) derivatives,²⁷ the tridentate 6-phenyl-2,2'-bipyridine ($\text{C}^{\wedge}\text{N}^{\wedge}\text{N}$) and its derivatives represent another attractive class of cyclometalating ligands to be coordinated to the gold(III) metal center.²⁹ In fact, the $\text{C}^{\wedge}\text{N}^{\wedge}\text{N}$ ligand system has been extensively employed for the preparation of luminescent platinum(II) complexes,^{30–33} yet reports on the related gold(III)- $\text{C}^{\wedge}\text{N}^{\wedge}\text{N}$ system are very scarce.^{34–36} It is envisaged that the utilization of different cyclometalating $\text{RC}^{\wedge}\text{N}^{\wedge}\text{N}$

Received: January 19, 2012

Published: June 25, 2012

ligands in combination with the σ -donating alkynyl ligands could lead to a substantial change in the frontier molecular orbital energies of the resulting complexes, thereby contributing to a class of novel gold(III) complexes with diverse luminescence properties. While an independent study on the synthesis and luminescence properties of the same class of alkyngold(III) complexes has appeared very recently,³⁶ the present work provides a comprehensive study of the photophysical properties of this class of compounds and valuable guiding principles on the design of this class of complexes with tunable emission energies. Herein we report the synthesis, characterization, electrochemistry, and photophysical study of a versatile class of luminescent cyclometalated alkyngold(III) complexes containing various tridentate RC[^]N[^]N ligands, [Au(RC[^]N[^]N)(C \equiv C–R[^])]PF₆. Computational studies have also been performed to provide insights into the nature of the excited states that led to the luminescence properties of these complexes, which would provide guiding principles on the design of this class of complexes with tunable emission energies.

EXPERIMENTAL SECTION

Materials and Reagents. Potassium tetrachloroaurate(III) was purchased from ChemPur. Tetra-*n*-butylammonium hexafluorophosphate and ammonium hexafluorophosphate were obtained from Strem Inc. The chlorogold(III) precursor complexes, [Au(RC[^]N[^]N)Cl]OTf,^{34b} were prepared according to a literature procedure, using different cyclometalating RC[^]N[^]N ligands synthesized by the Kröhnke procedure for pyridine synthesis.³⁷ *n*-Butyllithium (1.6 M in hexanes) was obtained from Acros, while 4-methoxyphenylacetylene, 4-(trifluoromethyl)phenylacetylene, 4-ethylphenylacetylene, and 3,3-dimethylbutyne were from Sigma-Aldrich. 1-Naphthylacetylene was prepared according to a reported procedure.³⁸ All solvents were purified and distilled using standard procedures before use. All other reagents were of analytical grade and used as received. Tetra-*n*-butylammonium hexafluorophosphate (Aldrich) was recrystallized twice from absolute ethanol before use.

Physical Measurements and Instrumentation. UV–Visible spectra were obtained on a Hewlett-Packard 8452A diode array spectrophotometer. ¹H NMR spectra were recorded on a Bruker DPX-300 (300 MHz) or Bruker DPX-400 (400 MHz) Fourier transform NMR spectrometer with chemical shifts recorded relative to tetramethylsilane (Me₄Si). Positive FAB mass spectra were recorded on a Thermo Scientific DFS High Resolution Magnetic Sector Mass Spectrometer. Elemental analyses for the metal complexes were performed on the Carlo Erba 1106 elemental analyzer at the Institute of Chemistry, Chinese Academy of Sciences in Beijing. Steady-state excitation and emission spectra were recorded on a Spex Fluorolog-2 model F111 fluorescence spectrofluorometer equipped with a Hamamatsu R-928 photomultiplier tube. Photophysical measurements in low-temperature glass were carried out with the sample solution loaded in a quartz tube inside a quartz-walled Dewar flask. Liquid nitrogen was placed into the Dewar flask for low temperature (77 K) photophysical measurements. Excited-state lifetimes of glass and solid samples were measured using a conventional laser system. The excitation source used was the 355-nm output (third harmonic, 8 ns) of a Spectra-Physics Quanta-Ray Q-switched GCR-150 pulsed Nd:YAG laser (10 Hz). Luminescence quantum yields of thin films were measured on a Hamamatsu C9920-03 Absolute PL Quantum Yield Measurement System. Cyclic voltammetric measurements were performed by using a CH Instruments, Inc. model CHI 600A electrochemical analyzer. The electrolytic cell used was a conventional two-compartment cell. Electrochemical measurements were performed in acetonitrile solutions with 0.1 M ⁿBu₄NPF₆ as supporting electrolyte at room temperature. The reference electrode was a Ag/AgNO₃ (0.1 M in acetonitrile) electrode, and the working electrode was a glassy carbon electrode (CH Instruments, Inc.) with a platinum wire as the

counter electrode. The working electrode surface was first polished with a 1- μ m alumina slurry (Linde), followed by a 0.3- μ m alumina slurry, on a microcloth (Buehler Co.). The ferrocenium/ferrocene couple (FeCp₂^{+/0}) was used as the internal reference.³⁹ All solutions for electrochemical studies were deaerated with prepurified argon gas just before measurements.

Crystal Structure Determination. Single crystals of **4** suitable for X-ray diffraction studies were grown by diffusion of diethyl ether vapor into a concentrated acetonitrile solution of the complex. The X-ray diffraction data were collected on a Bruker Smart CCD 1000, using graphite monochromatized Mo–K α radiation ($\lambda = 0.71073$ Å). The structure was solved by direct methods employing the SHELXS-97 program.⁴⁰ Full-matrix least-squares refinement on F^2 was used in the structure refinement. The positions of H atoms were calculated based on the riding mode with thermal parameters equal to 1.2 times those of the associated C atoms and participated in the calculation of final *R*-indices. In the final stage of least-squares refinement, all non-hydrogen atoms were refined anisotropically.

Synthesis. General Procedure for Syntheses of Alkyngold(III) Complexes. To a solution of alkyne (0.60 mmol) in tetrahydrofuran (30 mL) under a nitrogen atmosphere was added *n*-butyllithium (0.72 mmol, 1.6 M in hexanes) in a dropwise manner at –78 °C. The resulting mixture was stirred for 5 min and transferred to a suspension of [Au(RC[^]N[^]N)Cl]OTf (0.30 mmol) in tetrahydrofuran (30 mL). The reaction mixture was stirred for 3 h at room temperature, after which excess ammonium hexafluorophosphate (1.0 mmol) was added, and the resulting mixture was stirred for another hour at room temperature. Upon completion of reaction, the mixture was quenched by the addition of saturated ammonium chloride solution (1 mL). The crude product, which was obtained upon removal of solvent from the reaction mixture, was washed with dichloromethane to remove any organic impurities, and then with diethyl ether, followed by extraction with acetonitrile. The acetonitrile extract was concentrated, and subjected to filtration using a plastic syringe fitted with a disposable 0.2 μ m PTFE filter tip, and subsequent recrystallization by slow diffusion of diethyl ether vapor. The desired complex was obtained as yellow solids.

[Au(MeOC[^]N[^]N)(C \equiv C–C₆H₄–OCH₃-*p*)]PF₆ **1** (MeOHC[^]N[^]N = 6-(4-methoxyphenyl)-2,2'-bipyridine). This was prepared from [Au(MeOC[^]N[^]N)Cl]OTf (193 mg) and 4-methoxyphenylacetylene (79 mg) according to the general procedure. The titled complex was obtained as a yellow solid. Yield: 36 mg (16%). ¹H NMR (400 MHz, CD₃CN, 298 K, relative to Me₄Si): δ 3.82 (s, 3H, –OCH₃), 3.87 (s, 3H, –OCH₃), 6.90 (m, 3H, –C₆H₄– and C[^]N[^]N), 7.15 (m, 1H, C[^]N[^]N), 7.33 (d, *J* = 8.6 Hz, 2H, –C₆H₄–), 7.61 (d, *J* = 8.6 Hz, 1H, C[^]N[^]N), 7.83 (t, *J* = 8.0 Hz, 2H, C[^]N[^]N), 8.00 (d, *J* = 8.0 Hz, 1H, C[^]N[^]N), 8.20 (m, 1H, C[^]N[^]N), 8.33 (m, 2H, C[^]N[^]N), 8.86 (m, 1H, C[^]N[^]N); positive FAB-MS: *m/z* 589 [M–PF₆]⁺; IR (KBr): 2145 cm^{–1} (ν (C \equiv C)); elemental analyses calcd for C₂₆H₂₀AuF₆N₂O₂P·3H₂O (found): C 39.61 (39.78), H 3.32 (2.97), N 3.55 (3.91).

[Au(MeOC[^]N[^]N)(C \equiv C–C₆H₄–CF₃-*p*)]PF₆ **2**. This was prepared from [Au(MeOC[^]N[^]N)Cl]OTf (193 mg) and 4-(trifluoromethyl)phenylacetylene (102 mg) according to the general procedure. The titled complex was obtained as a yellow solid. Yield: 30 mg (13%). ¹H NMR (400 MHz, CD₃CN, 298 K, relative to Me₄Si): δ 3.89 (s, 3H, –OCH₃), 6.99 (m, 1H, C[^]N[^]N), 7.38 (m, 1H, C[^]N[^]N), 7.73 (m, 5H, –C₆H₄– and C[^]N[^]N), 7.95 (m, 2H, C[^]N[^]N), 8.10 (d, *J* = 8.0 Hz, 1H, C[^]N[^]N), 8.30 (t, *J* = 8.0 Hz, 1H, C[^]N[^]N), 8.42 (d, *J* = 8.0 Hz, 1H, C[^]N[^]N), 9.04 (d, *J* = 8.0 Hz, 1H, C[^]N[^]N); positive FAB-MS: *m/z* 627 [M–PF₆]⁺; IR (KBr): 2160 cm^{–1} (ν (C \equiv C)); elemental analyses calcd for C₂₆H₁₇AuF₉N₂OP·H₂O (found): C 39.51 (39.82), H 2.42 (2.31), N 3.54 (3.71).

[Au(MeC[^]N[^]N)(C \equiv C–C₆H₄–OCH₃-*p*)]PF₆ **3** (MeHC[^]N[^]N = 6-(4-tolyl)-2,2'-bipyridine). This was prepared from [Au(MeC[^]N[^]N)Cl]OTf (188 mg) and 4-methoxyphenylacetylene (79 mg) according to the general procedure. The titled complex was obtained as a yellow solid. Yield: 47 mg (22%). ¹H NMR (300 MHz, CD₃CN, 298 K, relative to Me₄Si): δ 2.09 (s, 3H, –CH₃), 3.87 (s, 3H, –OCH₃), 6.84 (d, *J* = 8.6 Hz, 2H, –C₆H₄–), 7.00 (m, 2H, C[^]N[^]N), 7.10 (d, *J* = 8.6

H_z, 2H, -C₆H₄-), 7.33 (d, *J* = 7.9 Hz, 1H, C[^]N[^]N), 7.65 (m, 2H, C[^]N[^]N), 7.87 (d, *J* = 7.9 Hz, 1H, C[^]N[^]N), 8.06–8.25 (m, 3H, C[^]N[^]N), 8.63 (d, *J* = 8.6 Hz, 1H, C[^]N[^]N); positive FAB-MS: *m/z* 573 [M-PF₆]⁺; IR (KBr): 2152 cm⁻¹ (ν(C≡C)); elemental analyses calcd for C₂₆H₂₀AuF₆N₂OP·2H₂O (found): C 41.39 (41.44), H 3.21 (3.01), N 3.71 (4.05).

[Au(MeC[^]N[^]N)(C≡C-C₆H₄-C₂H₅-p)]PF₆ **4**. This was prepared from [Au(MeC[^]N[^]N)Cl]OTf (188 mg) and 4-ethylphenylacetylene (78 mg) according to the general procedure. The titled complex was obtained as a yellow solid. Yield: 40 mg (18%). ¹H NMR (300 MHz, CD₃CN, 298 K, relative to Me₄Si): δ 1.26 (t, *J* = 7.6 Hz, 3H, -CH₃ of ethyl), 2.39 (s, 3H, -CH₃), 2.70 (q, 2H, -CH₂- of ethyl), 7.26 (d, *J* = 8.0 Hz, 3H, -C₆H₄- and C[^]N[^]N), 7.48 (d, *J* = 8.0 Hz, 2H, -C₆H₄-), 7.64 (m, 2H, C[^]N[^]N), 7.92 (m, 1H, C[^]N[^]N), 8.01 (d, *J* = 8.0 Hz, 1H, C[^]N[^]N), 8.15 (d, *J* = 8.0 Hz, 1H, C[^]N[^]N), 8.32 (t, *J* = 8.0 Hz, 1H, C[^]N[^]N), 8.41 (d, *J* = 8.0 Hz, 2H, C[^]N[^]N), 9.03 (d, *J* = 8.0 Hz, 1H, C[^]N[^]N); positive FAB-MS: *m/z* 571 [M-PF₆]⁺; IR (KBr): 2152 cm⁻¹ (ν(C≡C)); elemental analyses calcd for C₂₇H₂₂AuF₆N₂P·2H₂O (found): C 43.10 (43.17), H 3.48 (2.99), N 3.72 (3.72).

[Au(MeC[^]N[^]N)(C≡C-^{*i*}Bu)]PF₆ **5**. This was prepared from [Au(MeC[^]N[^]N)Cl]OTf (188 mg) and 3,3-dimethylbutyne (49 mg) according to the general procedure. The titled complex was obtained as a yellow solid. Yield: 28 mg (14%). ¹H NMR (300 MHz, CD₃CN, 298 K, relative to Me₄Si): δ 1.40 (s, 9H, ^{*i*}Bu), 2.42 (s, 3H, -CH₃), 7.28 (d, *J* = 8.2 Hz, 1H, C[^]N[^]N), 7.66 (m, 2H, C[^]N[^]N), 7.98 (m, 1H, C[^]N[^]N), 8.05 (d, *J* = 8.2 Hz, 1H, C[^]N[^]N), 8.17 (d, *J* = 8.2 Hz, 1H, C[^]N[^]N), 8.35 (t, *J* = 8.2 Hz, 1H, C[^]N[^]N), 8.43 (d, *J* = 8.2 Hz, 2H, C[^]N[^]N), 8.95 (d, *J* = 8.2 Hz, 1H, C[^]N[^]N); positive FAB-MS: *m/z* 523 [M-PF₆]⁺; IR (KBr): 2122 cm⁻¹ (ν(C≡C)); elemental analyses calcd for C₂₃H₂₂AuF₆N₂P (found): C 41.33 (41.37), H 3.32 (3.42), N 4.19 (4.26).

[Au(MeC[^]N[^]N)(C≡C-Np)]PF₆ **6**. This was prepared from [Au(MeC[^]N[^]N)Cl]OTf (188 mg) and 1-naphthylacetylene (91 mg) according to the general procedure. The titled complex was obtained as a yellow solid. Yield: 33 mg (15%). ¹H NMR (400 MHz, CD₃CN, 298 K, relative to Me₄Si): δ 2.37 (s, 3H, -CH₃), 7.24 (d, *J* = 8.1 Hz, 1H, C[^]N[^]N), 7.44 (t, *J* = 8.1 Hz, 1H, naphthyl), 7.56 (m, 3H, naphthyl), 7.62 (m, 2H, C[^]N[^]N), 7.82 (m, 2H, naphthyl), 7.91 (m, 3H, naphthyl and C[^]N[^]N), 8.14 (m, 1H, C[^]N[^]N), 8.19 (m, 1H, C[^]N[^]N), 8.29 (m, 2H, C[^]N[^]N), 8.94 (m, 1H, C[^]N[^]N); positive FAB-MS: *m/z* 559 [M-PF₆]⁺; IR (KBr): 2137 cm⁻¹ (ν(C≡C)); elemental analyses calcd for C₂₉H₂₀AuF₆N₂P·2H₂O (found): C 44.98 (44.99), H 3.12 (3.17), N 3.62 (3.43).

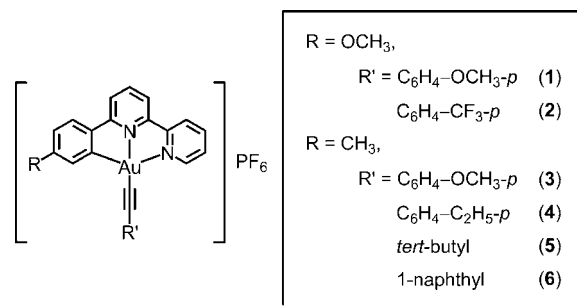
Computational Details. Calculations were carried out using Gaussian 03 software package.⁴¹ Geometry optimizations were performed for the ground-state structures of the complex cation [Au(RC[^]N[^]N)(C≡C-R)]⁺ (1'-6') with no symmetry restriction by using the density functional theory (DFT) at the hybrid Perdew, Burke, and Ernzerhof functional (PBE0) level of theory⁴² with a pruned (99,590) grid. On the basis of the ground state optimized geometries in the gas phase, non-equilibrium time-dependent density functional theory (TDDFT) method⁴³ at the same level associated with conductor-like polarizable continuum model (CPCM)⁴⁴ using CH₃CN as the solvent was employed to compute the singlet-singlet and singlet-triplet transitions for all the complexes. The unrestricted UPBE0 was used to optimize the first triplet excited state of complexes **2'** and **5'**. The Stuttgart effective core potentials (ECPs) and the associated basis set were applied to describe for Au⁴⁵ with f-type polarization functions (ζ = 1.050),⁴⁶ while the 6-31G(d,p) basis set⁴⁷ was used for all other atoms. Vibrational frequency calculations were performed for all stationary points to verify that each was a minimum (NIMAG = 0) on the potential energy surface. Mulliken population analyses were performed using MullPop.⁴⁸

RESULTS AND DISCUSSION

Synthesis and Characterization. All chlorogold(III) precursor complexes, [Au(RC[^]N[^]N)Cl]OTf,^{34b} were prepared according to the literature using various cyclometalating RC[^]N[^]N ligands synthesized by the procedure reported by

Kröhnke.³⁷ The alkynylgold(III) complexes **1–6** (Chart 1) were prepared by reacting the respective chlorogold(III)

Chart 1



precursor compound with various alkynyllithium reagents, prepared *in situ* from *n*-butyllithium and the respective alkynes in tetrahydrofuran under a nitrogen atmosphere at -78 °C. All the complexes are found to be air-stable upon storage in the dark. However, the complexes would readily decompose by reductive elimination in the presence of chlorinated solvents or upon prolonged heating. These cationic complexes are found to be very soluble in polar organic solvents such as acetonitrile and acetone, but poorly soluble in dichloromethane and chloroform, in contrast to the related neutral C[^]N[^]C-type alkynylgold(III) complexes.²⁶ The identities of all the complexes, namely, **1–6**, have been confirmed by ¹H NMR spectroscopy, FAB-mass spectrometry, and satisfactory elemental analyses. Their IR spectra exhibited a ν(C≡C) absorption at 2122–2160 cm⁻¹, which is in accordance with the presence of the alkyne ligand. In addition, the crystal structure of **4** has been determined by X-ray crystallography.

X-ray Crystal Structure. Single crystals of **4** were obtained by diffusion of diethyl ether vapor into a concentrated acetonitrile solution of the complex, and its structure was determined by X-ray crystallography. Crystal structure determination data are summarized in Table 1. The selected bond distances and bond angles are tabulated in Table 2. The perspective view of the crystal structure of **4** is depicted in Figure 1. The gold(III) metal center coordinates to the tridentate cyclometalating MeC[^]N[^]N ligand with the remaining site occupied by an alkyne ligand to give a distorted square-planar geometry, characteristic of d⁸ metal complexes. The C(16)–Au–N(2) angle of 82.0° and the N(1)–Au–N(2) angle of 78.9° about the gold(III) metal center are found to deviate from the ideal 90° owing to the restricted bite angle of the tridentate MeC[^]N[^]N ligand. The [Au(MeC[^]N[^]N)] motif is essentially coplanar, and the Au–C(16) (2.023 Å) and Au–N (1.997–2.123 Å) bond distances are similar to those found in other related complexes.^{26–28,35} The Au–C≡C and C≡C–C angles of 179.2° and 177.6° only deviate a little from the ideal 180°, establishing a slightly distorted linear arrangement, with the Au–C (1.990 Å) and C≡C bond distances (1.166 Å) similar to those found in the related cyclometalated alkynylgold(III) systems.^{26,27} Interestingly, the shortest Au···Au distance between adjacent molecules was found to be 3.6018 Å, suggestive of some weak aurophilic interactions, as the value was smaller than the Au(III)···Au(III) distances of 3.7 Å predicted by Pyykkö and co-workers.^{2b} Similar observations have also been reported very recently in related alkynylgold(III) complexes.³⁶ The molecules are arranged in a head-to-tail

Table 1. Crystal and Structure Determination Data of 4

[Au(MeC [^] N [^] N)(C≡C–C ₆ H ₄ –C ₂ H ₅ –p)]PF ₆ (4)	
empirical formula	C ₂₇ H ₂₂ AuF ₆ N ₂ P
formula weight	716.40
temp, K	293(2)
wavelength, Å	0.71073
crystal system	monoclinic
space group	P2 ₁ /n
a, Å	7.8064(11)
b, Å	14.564(2)
c, Å	22.853(3)
α, deg	90
β, deg	99.290(2)
γ, deg	90
volume, cm ³	2564.1(6)
Z, Å ³	4
density (calcd), g cm ⁻³	1.856
crystal size	0.29 mm × 0.07 mm × 0.06 mm
index ranges	–9 ≤ h ≤ 8 –16 ≤ k ≤ 17 –25 ≤ l ≤ 27
reflections collected/unique	13944/4515
GOF on F ²	0.873
final R indices [I > 2σ(I)]	R ₁ = 0.0357 wR ₂ = 0.1079
largest diff peak and hole, e Å ⁻³	1.210 and –0.714

Table 2. Selected Bond Lengths (Å) and Angles (deg) for 4^a

[Au(MeC [^] N [^] N)(C≡C–C ₆ H ₄ –C ₂ H ₅ –p)]PF ₆ (4)		
Bond Lengths (Å)		
Au(1)–C(18)		1.990(8)
Au(1)–C(16)		2.023(7)
Au(1)–N(2)		1.997(5)
Au(1)–N(1)		2.123(6)
C(18)–C(19)		1.166(9)
Bond Angles (deg)		
N(1)–Au(1)–C(16)		160.8(3)
N(2)–Au(1)–C(18)		178.3(2)
Au(1)–C(18)–C(19)		179.2(7)
N(2)–Au(1)–N(1)		78.9(2)
N(2)–Au(1)–C(16)		82.0(3)
C(18)–C(19)–C(20)		177.6(8)

^aWith estimated standard deviations (esds) given in parentheses.

fashion in the crystal lattice, with π – π stacking interactions of 3.441 Å between the [Au(MeC[^]N[^]N)] moiety and the aryl ring of the alkynyl ligand of the adjacent molecule. The crystal packing diagram is depicted in Figure 2.

Electrochemistry. The cyclic voltammograms of 1–6 in acetonitrile (0.1 mol dm⁻³ nBu₄NPF₆) generally show one quasi-reversible reduction couple at –0.87 to –0.93 V (vs SCE) and irreversible oxidation waves in the range of +1.50 to +1.99 V (vs SCE). The electrochemical data are summarized in Table 3. With reference to electrochemical studies of related alkynylgold(III) complexes,^{26,27} the reduction waves are tentatively assigned to a RC[^]N[^]N-centered reduction. In general, similar reduction potentials are observed for complexes with the same RC[^]N[^]N ligand.

On the other hand, the potentials for the oxidation waves are quite sensitive to the nature of the alkynyl ligand. In view of the redox-inactive nature of the gold(III) metal center, the

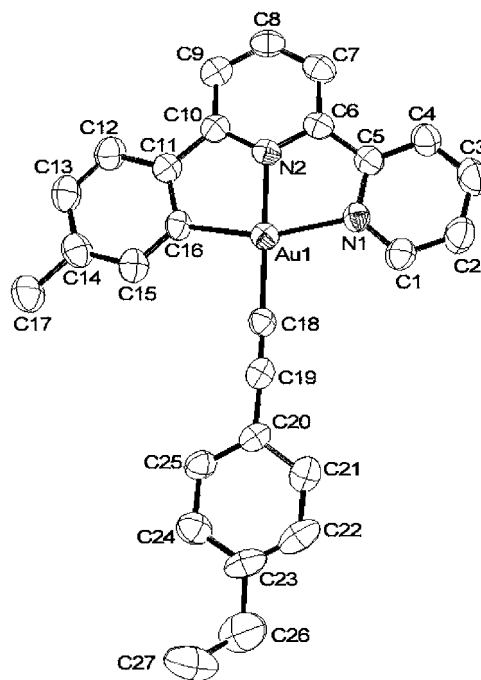


Figure 1. Perspective drawing of the complex cation of 4 with atomic numbering scheme. Hydrogen atoms are omitted for clarity. Thermal ellipsoids are drawn at the 30% probability level.

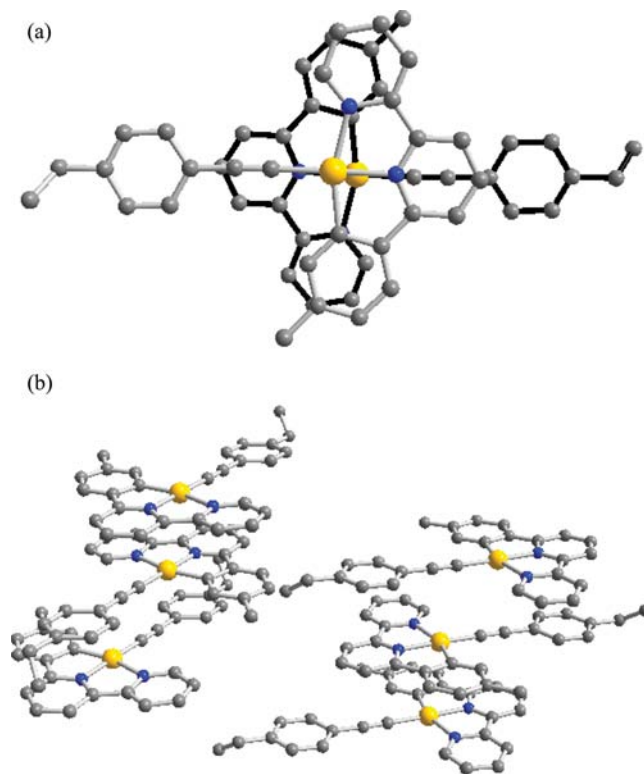


Figure 2. Crystal packing diagram of the complex cation of 4, showing (a) the “dimeric” configuration and (b) the extended array.

oxidation wave is assigned as the alkynyl ligand-centered oxidation, as in the related cyclometalated alkynylgold(III) complexes.^{26,27} Complexes with the same alkynyl groups generally show similar potentials. Complex 2, which contains the electron-withdrawing trifluoromethyl substituent on the

Table 3. Electrochemical Data for 1–6^a

complex	oxidation E_{pa}^b/V vs SCE	reduction $E_{1/2}^c/V$ vs SCE
1	+1.51	−0.90
2	+1.99	−0.87
3	+1.50	−0.89
4	+1.75	−0.93
5	-	−0.92
6	+1.59	−0.88

^aIn acetonitrile solution with 0.1 M ⁿBu₄NPF₆ as supporting electrolyte at room temperature; scan rate 100 mV s^{−1}. ^b E_{pa} refers to the anodic peak potential for the irreversible oxidation waves. ^c $E_{1/2} = (E_{pa} + E_{pc})/2$; E_{pa} and E_{pc} are peak anodic and peak cathodic potentials, respectively.

aryl alkynyl ligand, exhibits the most positive potential of +1.99 V vs SCE.

UV–Visible Absorption Spectroscopy. The UV–visible absorption spectra of complexes 1–6 in acetonitrile at 298 K all exhibit intense absorption in the higher energy region at wavelengths shorter than 320 nm, and a moderately intense broad absorption band at about 374–406 nm with extinction coefficients (ϵ) on the order of 10³ dm³ mol^{−1} cm^{−1}. The photophysical data of 1–6 are summarized in Table 4, and the

Table 4. Photophysical Data for 1–6

complex	absorption		emission		Φ_{em}
	λ_{max}/nm (ϵ_{max}/dm^3 $mol^{-1} cm^{-1}$)	medium (T/K)	λ_{max}/nm ($\tau_0/\mu s$)		
1	398 (6890) ^a	glass (77) ^{c,d}	514, 547 (260)		0.09
	400 (4290) ^b	solid (77)	566, 582 (77)		
		thin film (298) ^e	542		
2	406 (5710) ^a	glass (77) ^{c,d}	515, 550 (472)		0.13
	406 (4960) ^b	thin film (298) ^e	541		
3	380 (8240) ^a	glass (77) ^{c,d}	476, 509, 545sh (164)		0.12
	380 (6280) ^b	solid (77)	539 (104)		
		thin film (298) ^e	542		
4	374 (7870) ^a	glass (77) ^{c,d}	474, 507, 542 (274)		0.12
		thin film (298) ^f	549		
5	380 (6580) ^a	glass (77) ^{c,d}	469, 502, 537 (406)		0.22
		thin film (298) ^e	538		
6	378 (5445) ^a	glass (77) ^{c,d}	534, 576, 629sh (993)		0.13
	380 (5915) ^b	solid (77)	575, 615 (207)		
		thin film (298) ^e	546		

^aIn acetonitrile at 298 K. ^bIn acetone at 298 K. ^cVibronic-structured emission band. ^dMeasured in butyronitrile. ^e4% in MCP. ^f8% in MCP.

selected electronic absorption spectra of 1 and 3 are depicted in Figure 3. In general, complexes with the same cyclometalating ligand have been found to display absorption bands at similar energies. In the presence of electron-donating methoxy substituent on the phenyl moiety of the RC[^]N[^]N ligand, complexes 1 and 2 display an absorption band at about 398–406 nm. The presence of the weaker electron-donating methyl substituent in complexes 3–6 causes a blue shift in absorption energy to about 374–380 nm. Because of the sensitivity of the absorption energies to the nature of the cyclometalating RC[^]N[^]N ligands, it can be deduced that the excited state would involve some RC[^]N[^]N character. With reference to the electronic absorption studies of a related chlorogold(III)

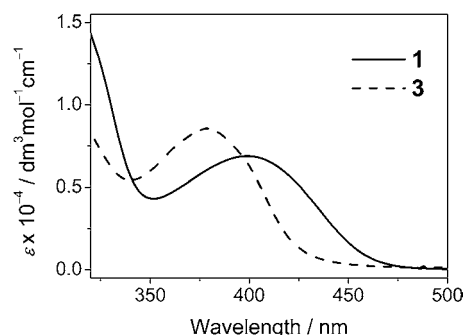


Figure 3. Electronic absorption spectra of 1 and 3 in acetonitrile at 298 K.

RC[^]N[^]N complex,^{34b} the lower-energy band of complexes 1–6 is tentatively assigned as the metal-perturbed intraligand $\pi-\pi^*$ transition of the RC[^]N[^]N ligand in the complexes, probably involving some charge transfer character from the aryl moiety to the bipyridine moiety of the cyclometalating ligand. Electronic absorption studies have also been performed in acetone solution at 298 K for complexes 1, 2, 3, and 6. It has been found that variation of the solvent has caused negligible change in the absorption energies and the band shapes, as well as minor changes in the extinction coefficients, further supporting the assignment of the low-energy absorption band.

Luminescence Spectroscopy. This class of gold(III) compounds is found to exhibit rich luminescence. The photophysical data of 1–6 are summarized in Table 4. Attempts have been made to measure the room temperature solution emission in acetonitrile as well as in acetone. However, the complexes are found to be rather unstable in the solution state, probably because of photodecomposition and/or other side reactions. On the other hand, the complexes have been observed to be highly emissive at low temperature in glass matrices as well as in the solid state at 77 K. In butyronitrile glass at 77 K (concentration = $\sim 10^{-4}$ M), the complexes have been found to exhibit vibronically structured emission bands at 469–629 nm (Figure 4). The vibrational progressional

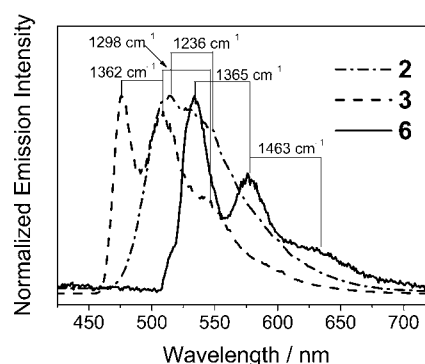


Figure 4. Normalized emission spectra of 2, 3, and 6 in butyronitrile glass at 77 K.

spacings, ranging from 1173 to 1402 cm^{−1}, are in line with the C=C and C=N vibrational modes of the RC[^]N[^]N ligand. With the exception of complex 6, the emission is assigned as the emission bands originated from the intraligand (IL) states of the cyclometalating RC[^]N[^]N ligand, with some charge transfer character from the aryl moiety to the bipyridine moiety. With the more electron-donating methoxy substituents

attached to the phenyl unit of the RC[^]N[^]N ligand in complexes **1** and **2**, the $\pi(\text{RC}^{\wedge}\text{N}^{\wedge}\text{N})$ orbital would be raised to a larger extent than the $\pi^*(\text{RC}^{\wedge}\text{N}^{\wedge}\text{N})$ orbital relative to those in complexes **3–6**, leading to the reduction in π – π^* energy separation and thus the red shift in emission of complexes **1** and **2**. Complex **6**, on the other hand, has been observed to exhibit an exceptionally low-energy, vibronic-structured emission band with emission maximum at 534 nm with vibrational progressional spacings of 1365–1463 cm⁻¹. This emission is tentatively assigned as derived from the ³IL π – π^* state of the naphthyl alkynyl ligand. Such assignments have been further supported by TDDFT calculation (vide infra). The butyronitrile glass emission of one of the precursor complexes, namely, [Au(MeC[^]N[^]N)Cl]OTf, has also been studied. The precursor complex is found to exhibit vibronically structured emission bands with energies very similar to that of the respective alkynyl complexes **3–5**, which can be assigned as the IL emission of the MeC[^]N[^]N moiety. This resemblance in emission between the alkynylgold(III) complexes and their respective chlorogold(III) precursors can confirm the IL assignment of the vibronically structured emission bands of complexes **1–5**.

Complexes **1–6** all exhibit moderately intense emission in solid-state thin films when doped into 1,3-bis(9*H*-carbazol-9-yl)benzene (MCP) at 298 K (Figure 5). The complexes have

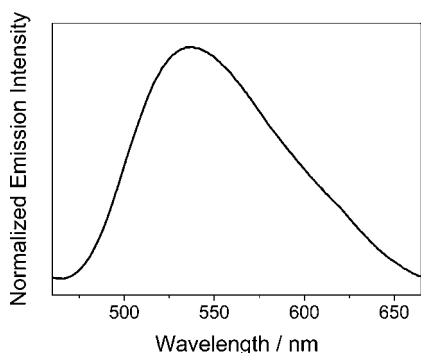


Figure 5. Normalized emission spectra of **5** in thin film (4% doped in MCP) at 298 K.

been observed to show a broad, structureless emission band at 538–549 nm. Since most of the complexes, that is, complexes **1–4** and **6**, display emission bands at similar energies at 541–549 nm, an intraligand origin of the cyclometalating ligand would be improbable. With reference to the solid state emission of related cyclometalated alkynylgold(III) complexes,²⁶ the thin film emission band of **1–6** at 538–549 nm is tentatively assigned to be attributed to the π – π excimeric ³IL emission because of the possible π – π stacking interaction of the RC[^]N[^]N ligand in the solid state thin film. The photoluminescence quantum yields of the MCP-doped thin films have been determined, with values ranging from 0.09 to 0.22. The solid state emission properties of selected complexes, namely, **1**, **3**, and **6**, have also been studied, and these complexes are found to be strongly emissive at 77 K, exhibiting emission bands at 539–615 nm, which can also be assigned as an excimeric emission resulted from the π – π stacking interactions of the cyclometalating ligand.

Computational Studies. DFT and TDDFT calculations at the PBE0 level of theory were performed to study the complex cations, [Au(RC[^]N[^]N)(C \equiv C–R)]⁺ shown in Chart 1 (**1'–6'**) to gain further insights into the nature of absorption and

emission origins of these complexes. Details of the optimized structures are given in the Supporting Information, Figure S1 and Table S1.

Selected singlet–singlet transitions for **1'–6'** are listed in Table 5. Several transitions are computed in the region of the low-energy absorption band. The spatial plots of TDDFT/CPCM molecular orbitals (MOs) involved in the transitions in **1'** are shown in Figure 6, and the percentage contributions of the MOs and orbital energies for all the complexes are listed in Supporting Information, Tables S2 and S3, respectively. The lowest-energy singlet–singlet transition in each of the complexes mainly corresponds to one-electron excitation from the highest occupied MO (HOMO) to the lowest unoccupied MO (LUMO). With the exception of the 4-(trifluoromethyl)phenyl- and *tert*-butyl-substituted alkynyl complexes (**2'** and **5'**), the lowest-energy transition for all the complexes can be assigned as ligand-to-ligand charge transfer transition (LLCT) from the π orbital of the aryl alkynyl ligand to the π^* orbital of the RC[^]N[^]N ligand localized on the bipyridine unit. For complexes **2'** and **5'**, the lowest-energy transition can be assigned as the IL π – π^* transition of the RC[^]N[^]N ligand, involving the excitation from the π orbital localized on the phenylpyridine unit to the π^* orbital localized on the bipyridine unit. A similar IL π – $\pi^*(\text{RC}^{\wedge}\text{N}^{\wedge}\text{N})$ transition is computed to be the S₀ → S₂ transition for **1'**, **3'** and **4'**, **6'**.

As shown in Table 5, the IL π – $\pi^*(\text{RC}^{\wedge}\text{N}^{\wedge}\text{N})$ transition is calculated to be more intense than the LLCT [$\pi(\text{C}\equiv\text{C}-\text{R}) \rightarrow \pi^*(\text{RC}^{\wedge}\text{N}^{\wedge}\text{N})$] transition for all the complexes and is computed to be red-shifted upon going from **3'–6'** (371–373 nm) to **1'–2'** (406 nm). Since the $\pi(\text{RC}^{\wedge}\text{N}^{\wedge}\text{N})$ orbital has a larger contribution of the phenyl π orbital than the $\pi^*(\text{RC}^{\wedge}\text{N}^{\wedge}\text{N})$ orbital (Supporting Information, Table S2), the $\pi(\text{RC}^{\wedge}\text{N}^{\wedge}\text{N})$ orbital is destabilized to a larger extent than the $\pi^*(\text{RC}^{\wedge}\text{N}^{\wedge}\text{N})$ orbital with the more electron-donating –OMe group attached to the phenyl unit. In general, the calculated wavelengths of the IL π – $\pi^*(\text{RC}^{\wedge}\text{N}^{\wedge}\text{N})$ transitions are in agreement with the observed trend in the low-energy absorption band.

Supporting Information, Table S4 lists the first two lowest-energy singlet–triplet transitions in **1'–6'**. For all the complexes with the exception of complex **6'**, the lowest-energy singlet–triplet transition is either the ³IL π – π^* transition of the RC[^]N[^]N ligand (**1'**, **2'**, **4'** and **5'**) or the ³LLCT [$\pi(\text{C}\equiv\text{C}-\text{R}) \rightarrow \pi^*(\text{RC}^{\wedge}\text{N}^{\wedge}\text{N})$] transition (**3'**). The ³IL π – $\pi^*(\text{RC}^{\wedge}\text{N}^{\wedge}\text{N})$ transition for **3'** is computed to be the S₀ → T₂ transition. Geometry optimization of the lowest-energy ³IL π – $\pi^*(\text{RC}^{\wedge}\text{N}^{\wedge}\text{N})$ triplet excited state for complexes **2'** and **5'** with the MeC[^]N[^]N and MeOC[^]N[^]N ligands, respectively, have been performed using the unrestricted Kohn–Sham approach (UPBE0).⁴² The plot of spin density of the ³IL triplet excited states reveal that the spin distribution for **2'** is somewhat different from **5'** (Figure 7), in which the spin density in **2'** is distributed over the entire RC[^]N[^]N unit.

Different from the other complexes, the lowest-energy singlet–triplet transition for **6'** is mainly attributed to the HOMO → LUMO+4 excitation. Since the LUMO+4 is the π^* orbital of the naphthyl alkynyl ligand, this transition can be assigned as ³IL π – π^* transition of the naphthyl alkynyl ligand. On the basis of DFT and TDDFT calculations as well as the observed trend of the emission λ_{max} and the vibronic-structured emission band, the emission at 77 K for **1–5** is originated from the ³IL π – $\pi^*(\text{RC}^{\wedge}\text{N}^{\wedge}\text{N})$ excited state while for complex **6**, is originated from the ³IL π – $\pi^*(\text{C}\equiv\text{C}-\text{Np})$ excited state.

Table 5. Selected Singlet–Singlet Transitions in 1'–6' Computed by TDDFT/CPCM Using CH₃CN as the Solvent

compound	transition	orbital involved ^a	coefficient	f^b	vertical excitation wavelength (nm)
1'	$S_0 \rightarrow S_1$	H \rightarrow L	0.70	0.054	455
	$S_0 \rightarrow S_2$	H-1 \rightarrow L	0.68	0.110	406
	$S_0 \rightarrow S_3$	H \rightarrow L+2	0.68	0.046	366
	$S_0 \rightarrow S_4$	H \rightarrow L+1	0.70	0.019	355
2'	$S_0 \rightarrow S_1$	H \rightarrow L	0.68	0.115	406
	$S_0 \rightarrow S_2$	H-1 \rightarrow L	0.70	0.000	372
	$S_0 \rightarrow S_3$	H \rightarrow L+2	0.70	0.000	337
	$S_0 \rightarrow S_4$	H-1 \rightarrow L+2	0.52	0.020	320
3'	$S_0 \rightarrow S_1$	H \rightarrow L	0.70	0.029	463
	$S_0 \rightarrow S_2$	H-1 \rightarrow L	0.57	0.066	373
	$S_0 \rightarrow S_3$	H \rightarrow L+2	0.56	0.096	366
	$S_0 \rightarrow S_4$	H \rightarrow L+1	0.68	0.015	365
4'	$S_0 \rightarrow S_1$	H \rightarrow L	0.70	0.000	425
	$S_0 \rightarrow S_2$	H-1 \rightarrow L	0.67	0.101	372
	$S_0 \rightarrow S_3$	H \rightarrow L+2	0.68	0.078	347
	$S_0 \rightarrow S_4$	H \rightarrow L+1	0.70	0.000	339
5'	$S_0 \rightarrow S_1$	H \rightarrow L	0.68	0.104	371
	$S_0 \rightarrow S_2$	H-1 \rightarrow L	0.70	0.000	343
	$S_0 \rightarrow S_3$	H-2 \rightarrow L	0.70	0.050	334
6'	$S_0 \rightarrow S_1$	H \rightarrow L	0.70	0.002	464
	$S_0 \rightarrow S_2$	H-1 \rightarrow L	0.58	0.079	373
	$S_0 \rightarrow S_3$	H \rightarrow L+2	0.50	0.088	366
	$S_0 \rightarrow S_4$	H \rightarrow L+1	0.60	0.027	365

^aThe orbitals involved in the major excitation (H = HOMO and L = LUMO). ^bOscillator strengths.

CONCLUSION

A novel class of luminescent cyclometalated alkynylgold(III) complexes has been synthesized and characterized. The X-ray

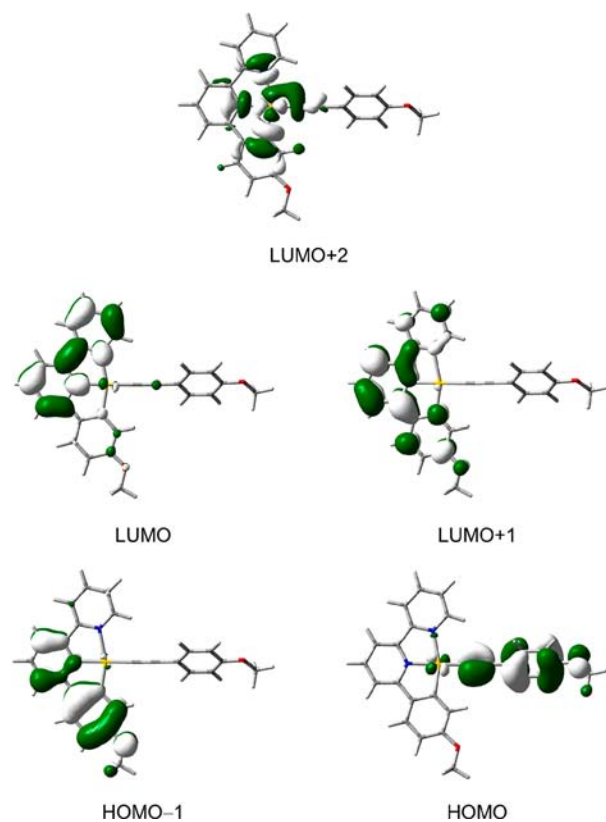


Figure 6. Spatial plots (isovalue = 0.03) of selected molecular orbitals in 1' obtained from the TDDFT/CPCM calculations.

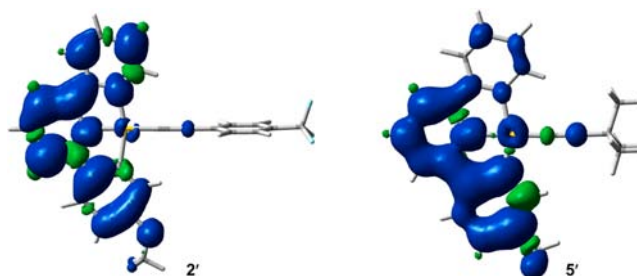


Figure 7. Plot of spin density (isovalue = 0.001) for the ³IL triplet excited state in 2' and 5'.

crystal structure of 4 has been determined. Electrochemical studies reveal a quasi-reversible reduction couple originating from the RC^NN ligands at -0.87 to -0.93 V (vs SCE) and irreversible alkynyl-centered oxidation waves in the range of $+1.50$ to $+1.99$ V (vs SCE). The electronic absorption and emission properties of the complexes have also been studied in detail. In acetonitrile at room temperature, the complexes show intense absorption at the higher energy region with wavelength shorter than 320 nm, and a moderately intense broad absorption band at 374–406 nm, assigned as the metal-perturbed intraligand π – π^* transition of the cyclometalating RC^NN ligand, with charge transfer character from the aryl ring to the bipyridine moiety. Most of the complexes have been observed to show vibronic-structured emission bands at 469–550 nm in butyronitile glass at 77 K, assigned to an intraligand excited state of the RC^NN ligand, with some charge transfer character from the aryl to the bipyridine moiety. The emission origin can be switched from the intraligand state of the cyclometalating ligand to the ³IL π – π^* state of the ancillary alkynyl ligand when 1-naphthylacetylene has been incorporated into the gold(III) metal center. TDDFT calculations have been performed, and the results are found to be in agreement with

the experimental observations. The photophysical and computational studies have provided a deeper understanding into the photoluminescence properties of this class of cyclometalated alkynylgold(III) complexes. In particular, the readiness in the fine-tuning of the photophysical properties in this system through employing a variety of cyclometalating ligands and ancillary alkynyl ligands has opened up new opportunities in the use of such organogold(III) complexes for novel applications and functions.

■ ASSOCIATED CONTENT

■ Supporting Information

Selected structural parameters of the optimized structures, percentage contribution of selected MOs, orbital energies, selected TDDFT/CPCM singlet–triplet transitions, optimized structures of **1'**, and Cartesian coordinates of the optimized structures. This material is available free of charge via the Internet at <http://pubs.acs.org>.

■ AUTHOR INFORMATION

Corresponding Author

*E-mail: wvyam@hku.hk.

Notes

The authors declare no competing financial interest.

■ ACKNOWLEDGMENTS

V.W.-W.Y. acknowledges support from The University of Hong Kong and the URC Strategic Research Theme on Molecular Materials. This work has been supported by the Theme-Based Research Scheme (T23-713/11) and the General Research Fund (GRF) (HKU 7063/10P), both from the Research Grants Council of Hong Kong Special Administrative Region, PR China. Dr. L. Szeto is gratefully acknowledged for technical assistance in crystal structure determination. Dr. K. M.-C. Wong is also acknowledged for helpful discussions. V. K.-M.A. acknowledges the receipt of a postgraduate studentship from The University of Hong Kong. The computational studies have been conducted using the HKU Computer Centre research computing facilities that are supported in part by the Hong Kong UGC Special Equipment Grant (SEG HKU09).

■ REFERENCES

- (1) (a) Balzani, V.; Bergamini, G.; Campagna, S.; Puntoriero, F. *Top. Curr. Chem.* **2007**, *280*, 1. (b) Kirgan, R. A.; Sullivan, B. P.; Rillema, D. P. *Top. Curr. Chem.* **2007**, *281*, 45. (c) Flamigni, L.; Barbieri, A.; Sabatini, C.; Ventura, B.; Barigelletti, F. *Top. Curr. Chem.* **2007**, *281*, 143. (d) Williams, J. A. G. *Top. Curr. Chem.* **2007**, *281*, 205. (e) Yam, V. W.-W.; Cheng, E. C.-C. *Top. Curr. Chem.* **2007**, *281*, 269.
- (2) (a) Pyykkö, P. *Chem. Rev.* **1988**, *88*, 563. (b) Mendizabal, F.; Pyykkö, P. *Phys. Chem. Chem. Phys.* **2004**, *6*, 900.
- (3) Ford, P. C.; Vogler, A. *Acc. Chem. Res.* **1993**, *26*, 220.
- (4) (a) Schmidbaur, H. *Chem. Soc. Rev.* **1995**, *24*, 391. (b) Hutchings, G. J.; Brust, M.; Schmidbaur, H. *Chem. Soc. Rev.* **2008**, *37*, 1759.
- (5) Fung, E. Y.; Olmstead, M. M.; Vickery, J. C.; Balch, A. L. *Coord. Chem. Rev.* **1998**, *171*, 151.
- (6) Schmidbaur, H., Ed.; *Gold: Progress in Chemistry, Biochemistry and Technology*; J. Wiley & Sons: Chichester, U. K., 1999.
- (7) (a) Yam, V. W.-W.; Lo, K. K.-W. *Chem. Soc. Rev.* **1999**, 323. (b) Yam, V. W.-W.; Cheng, E. C.-C. *Chem. Soc. Rev.* **2008**, *37*, 1806.
- (8) Vogler, A.; Kunkely, H. *Coord. Chem. Rev.* **2001**, *219–221*, 489.
- (9) Burini, A.; Mohamed, A. A.; Fackler, J. P., Jr. *Comments Inorg. Chem.* **2003**, *24*, 253.
- (10) Puddephatt, R. J. *Chem. Soc. Rev.* **2008**, *37*, 2012.

- (11) Laguna, A., Ed.; *Modern Supramolecular Gold Chemistry*; Wiley-VCH: Weinheim, Germany, 2008.
- (12) Mohr, F., Ed.; *Gold Chemistry: Applications and Future Directions in the Life Sciences*; Wiley-VCH: Weinheim, Germany, 2009.
- (13) Powell, C. E.; Humphrey, M. G. *Coord. Chem. Rev.* **2004**, *248*, 725.
- (14) Di Bella, S. *Chem. Soc. Rev.* **2001**, *30*, 355.
- (15) Wong, W.-Y.; Ho, C.-L. *Acc. Chem. Res.* **2010**, *43*, 1246.
- (16) Coe, B. J.; Curati, N. R. M. *Comments Inorg. Chem.* **2004**, *25*, 147.
- (17) Chi, Y.; Chou, P.-T. *Chem. Soc. Rev.* **2010**, *39*, 638.
- (18) Demas, J. N.; DeGraff, B. A. *Coord. Chem. Rev.* **2001**, *211*, 317.
- (19) Sun, S.-S.; Lees, A. J. *Coord. Chem. Rev.* **2002**, *230*, 171.
- (20) Wong, K. M.-C.; Tang, W.-S.; Chu, B. W.-K.; Zhu, N.; Yam, V. W.-W. *Organometallics* **2004**, *23*, 3459.
- (21) Fernández-Moreira, V.; Thorp-Greenwood, F. L.; Coogan, M. P. *Chem. Commun.* **2010**, *46*, 186.
- (22) Alonso-Vante, N. *ChemPhysChem* **2010**, *11*, 2732.
- (23) Teyssot, M.-L.; Jarrousse, A.-S.; Manin, M.; Chevry, A.; Roche, S.; Norre, F.; Beaudoin, C.; Morel, L.; Boyer, D.; Machiou, R.; Gautier, A. *Dalton Trans.* **2009**, 6894.
- (24) Knipp, M. *Curr. Med. Chem.* **2009**, *16*, 522.
- (25) Yam, V. W.-W.; Choi, S. W.-K.; Lai, T.-F.; Lee, W.-K. *J. Chem. Soc., Dalton Trans.* **1993**, 1001.
- (26) (a) Yam, V. W.-W.; Wong, K. M.-C.; Hung, L.-L.; Zhu, N. *Angew. Chem.* **2005**, *117*, 3167. (b) Wong, K. M.-C.; Zhu, X.; Hung, L.-L.; Zhu, N.; Yam, V. W.-W.; Kwok, H.-S. *Chem. Commun.* **2005**, 2906. (c) Wong, K. M.-C.; Hung, L.-L.; Lam, W. H.; Zhu, N.; Yam, V. W.-W. *J. Am. Chem. Soc.* **2007**, *129*, 4350. (d) Au, V. K.-M.; Wong, K. M.-C.; Tsang, D. P.-K.; Chan, M.-Y.; Zhu, N.; Yam, V. W.-W. *J. Am. Chem. Soc.* **2010**, *132*, 14273.
- (27) Au, V. K.-M.; Wong, K. M.-C.; Zhu, N.; Yam, V. W.-W. *Chem.—Eur. J.* **2011**, *17*, 130.
- (28) (a) Au, V. K.-M.; Wong, K. M.-C.; Zhu, N.; Yam, V. W.-W. *J. Am. Chem. Soc.* **2009**, *131*, 9076. (b) Yan, J. J.; Chow, A. L.-F.; Leung, C.-H.; Sun, R. W.-Y.; Ma, D.-L.; Che, C.-M. *Chem. Commun.* **2010**, *46*, 3893.
- (29) Au, V. K.-M. Ph. D. Thesis, The University of Hong Kong, 2012.
- (30) (a) Lai, S.-W.; Chan, M. C.-W.; Cheung, K.-K.; Che, C.-M. *Organometallics* **1999**, *18*, 3327. (b) Lai, S.-W.; Lam, H.-W.; Lu, W.; Cheung, K.-K.; Che, C.-M. *Organometallics* **2002**, *21*, 226. (c) Lu, W.; Mi, B.-X.; Chan, M. C. W.; Hui, Z.; Che, C.-M.; Zhu, N.; Lee, S.-T. *J. Am. Chem. Soc.* **2004**, *126*, 4958.
- (31) Neve, F.; Crispini, A.; Di Pietro, C.; Campagna, S. *Organometallics* **2002**, *21*, 3511.
- (32) Lanoë, P. H.; Le Bozec, H.; Williams, J. A. G.; Fillaut, J. L.; Guerschais, V. *Dalton Trans.* **2010**, *39*, 707.
- (33) (a) Shao, P.; Li, Y.; Yi, J.; Pritchett, T. M.; Sun, W. *Inorg. Chem.* **2010**, *49*, 4507. (b) Zhang, J.-F.; Gan, X.; Fu, W.-F.; Han, X.; Li, L. *Inorg. Chim. Acta* **2010**, *363*, 338.
- (34) (a) Chan, C.-W.; Wong, W.-T.; Che, C.-M. *Inorg. Chem.* **1994**, *33*, 1266. (b) Liu, H.-Q.; Cheung, T.-C.; Peng, S.-M.; Che, C.-M. *J. Chem. Soc., Chem. Commun.* **1995**, 1787.
- (35) (a) Cinellu, M. A.; Minghetti, G.; Pinna, M. V.; Stoccoro, S.; Zucca, A.; Manassero, M. *J. Chem. Soc., Chem. Commun.* **1998**, 2397. (b) Cinellu, M. A.; Minghetti, G.; Pinna, M. V.; Stoccoro, S.; Zucca, A.; Manassero, M. *J. Chem. Soc., Dalton Trans.* **1999**, 2823.
- (36) Lu, W.; Chan, K. T.; Wu, S.-X.; Chen, Y.; Che, C.-M. *Chem. Sci.* **2012**, *3*, 752.
- (37) Kröhnke, F. *Synthesis* **1976**, 1.
- (38) Neenan, T. X.; Whitesides, G. M. *J. Org. Chem.* **1988**, *53*, 2489.
- (39) Connelly, N. G.; Geiger, W. E. *Chem. Rev.* **1996**, *96*, 877.
- (40) Sheldrick, G. M. *SHELXS 97: Programs for Crystal Structure Analysis* (release 97-2); University of Göttingen: Göttingen, Germany, 1997.
- (41) Frisch, M. J.; Trucks, G. W.; Schlegel, H. B.; Scuseria, G. E.; Robb, M. A.; Cheeseman, J. R.; Montgomery, Jr., J. A.; Vreven, T.; Kudin, K. N.; Burant, J. C.; Millam, J. M.; Iyengar, S. S.; Tomasi, J.;

Barone, V.; Mennucci, B.; Cossi, M.; Scalmani, G.; Rega, N.; Petersson, G. A.; Nakatsuji, H.; Hada, M.; Ehara, M.; Toyota, K.; Fukuda, R.; Hasegawa, J.; Ishida, M.; Nakajima, T.; Honda, Y.; Kitao, O.; Nakai, H.; Klene, M.; Li, X.; Knox, J. E.; Hratchian, H. P.; Cross, J. B.; Bakken, V.; Adamo, C.; Jaramillo, J.; Gomperts, R.; Stratmann, R. E.; Yazyev, O.; Austin, A. J.; Cammi, R.; Pomelli, C.; Ochterski, J. W.; Ayala, P. Y.; Morokuma, K.; Voth, G. A.; Salvador, P.; Dannenberg, J. J.; Zakrzewski, V. G.; Dapprich, S.; Daniels, A. D.; Strain, M. C.; Farkas, O.; Malick, D. K.; Rabuck, A. D.; Raghavachari, K.; Foresman, J. B.; Ortiz, J. V.; Cui, Q.; Baboul, A. G.; Clifford, S.; Cioslowski, J.; Stefanov, B. B.; Liu, G.; Liashenko, A.; Piskorz, P.; Komaromi, I.; Martin, R. L.; Fox, D. J.; Keith, T.; Al-Laham, M. A.; Peng, C. Y.; Nanayakkara, A.; Challacombe, M.; Gill, P. M. W.; Johnson, B.; Chen, W.; Wong, M. W.; Gonzalez, C.; Pople, J. A. *Gaussian 03*, Revision E.01; Gaussian, Inc.: Wallingford, CT, 2004.

(42) (a) Perdew, J. P.; Burke, K.; Ernzerhof, M. *Phys. Rev. Lett.* **1996**, *77*, 3865. (b) Perdew, J. P.; Burke, K.; Ernzerhof, M. *Phys. Rev. Lett.* **1997**, *78*, 1396. (c) Adamo, C.; Barone, V. *J. Chem. Phys.* **1999**, *110*, 6158.

(43) (a) Stratmann, R. E.; Scuseria, G. E.; Frisch, M. J. *J. Chem. Phys.* **1998**, *109*, 8218. (b) Bauernschmitt, R.; Ahlrichs, R. *Chem. Phys. Lett.* **1996**, *256*, 454. (c) Casida, M. E.; Jamorski, C.; Casida, K. C.; Salahub, D. R. *J. Chem. Phys.* **1998**, *108*, 4439.

(44) (a) Barone, V.; Cossi, M. *J. Phys. Chem. A* **1998**, *102*, 1995. (b) Cossi, M.; Rega, N.; Scalmani, G.; Barone, V. *J. Comput. Chem.* **2003**, *24*, 669.

(45) Andrae, D.; Häussermann, U.; Dolg, M.; Stoll, H.; Preuss, H. *Theor. Chim. Acta* **1990**, *77*, 123.

(46) Ehlers, A. W.; Böhme, M.; Dapprich, S.; Gobbi, A.; Höllwarth, A.; Jonas, V.; Köhler, K. F.; Stegmann, R.; Veldkamp, A.; Frenking, G. *Chem. Phys. Lett.* **1993**, *208*, 111.

(47) (a) Hehre, W. J.; Ditchfield, R.; Pople, J. A. *J. Chem. Phys.* **1972**, *56*, 2257. (b) Hariharan, P. C.; Pople, J. A. *Theor. Chim. Acta* **1973**, *28*, 213. (c) Francl, M. M.; Pietro, W. J.; Hehre, W. J.; Binkley, J. S.; Gordon, M. S.; Defrees, D. J.; Pople, J. A. *J. Chem. Phys.* **1982**, *77*, 3654.

(48) Pis Diez, R. *MullPop*; National University of La Plata: La Plata, Buenos Aires, Argentina, 2003.

■ NOTE ADDED AFTER ASAP PUBLICATION

This paper was published on the Web on June 25, 2012. Additional corrections were added, including changes to the Au–Au distance and the addition of reference 2b. The corrected version was reposted on July 5, 2012.